Eur. J. Mineral.
2018, **30**, 859–868
Published online 9 May 2018

New data on cafarsite: reinvestigation of its crystal structure and chemical composition

GEORGIA CAMETTI[1,*], MARIKO NAGASHIMA[2], MARTIN FISCH[1] and THOMAS ARMBRUSTER[1]

[1] Mineralogical Crystallography, Institute of Geological Sciences, University of Bern, Baltzerstr. 1+3, 3012 Bern, Switzerland
*Corresponding author, e-mail: georgia.cametti@krist.unibe.ch
[2] Graduate School of Science and Engineering, Yamaguchi University, Yamaguchi 753-8512, Japan

Abstract: The crystal structure of cafarsite from Wanni glacier, Monte Cervandone, was re-investigated by single-crystal X-ray diffraction (space group $Pn\bar{3}$, $R1 = 0.022$) and new electron-microprobe analyses. The REE (mainly Ce and Y) were found to substitute Ca. A new anion site, four-coordinated by Ca, was located by difference Fourier analysis and refined with F scattering factors. Two octahedral sites (Ti1 and Fe2) are occupied by mainly Ti and Fe^{3+}, replacing each other whereas the octahedral site Mn1 hosts Mn^{2+} and Fe^{2+}. The new structure refinements and chemical analyses lead to the simplified chemical formula $(Ca_{7.8}Na_{0.8}Mn_{0.5}REE_{0.4})_{\Sigma 9.5}(Ti_{3.9}Fe^{3+}_{2.1}Fe^{2+}_{0.9}Mn^{2+}_{0.1})_{\Sigma 7}(AsO_3)_{14}F_{0.5}$. According to our findings, there is no evidence for either H_2O or OH in the structure. In contrast to the original study of 1977, the structure has no significant cation vacancies and is based on 14 AsO_3 groups per formula unit, not on 12 AsO_3 as previously suggested.

Key-words: cafarsite; crystal structure; electron-microprobe analyses; calcium titanium arsenite; new formula; REE.

1. Introduction

Cafarsite is a rare cubic (space group $Pn\bar{3}$) As-mineral, firstly reported by Graeser (1966) who characterized it from mineralized zones in two-mica leucocratic gneiss of the Monte Leone nappe outcropping in the Binntal, on the slopes of Monte Cervandone, at the Swiss-Italian border. The unique mineralization of rare minerals in this rock was tentatively related (Guastoni *et al.*, 2006) to interaction of As-rich hydrothermal fluids with pegmatites during the Alpine event. Cafarsite was initially described as an arsenate with chemical composition $Ca_{5.6}Fe_{3.3}Ti_{2.5}Mn_{1.7}O_{10}(As^{5+}O_4)_{12}{\cdot}4H_2O$. Subsequently, new chemical analyses coupled with structural investigation showed that cafarsite is actually an arsenite with idealized chemical formula $Ca_{5.9}Mn_{1.7}Ti_3Fe_3(As^{3+}O_3)_{12}{\cdot}4–5H_2O$ (Edenharter *et al.*, 1977). A second occurrence of cafarsite was reported from the Hemlo gold deposit, Ontario, Canada (Harris, 1989). In contrast to the Swiss-Italian locality, this material represents a Mn-rich variety with significant V content but low Fe.

The crystal structure of cafarsite was described as constituted by AsO_3 trigonal pyramids linked to $M\phi_{4–6}$ polyhedra, with M = *Ca*, Ti, Fe, and Mn. Although the mineral was considered to be hydrated (Graeser, 1966; Edenharter *et al.*, 1977) a position of the H_2O molecule was not located in the refined structure and, most intriguing, no space for hosting potential H_2O molecules was available in their structure model (Edenharter *et al.*, 1977).

This study was initiated to clarify this contradiction and to determine whether H_2O is actually present in cafarsite. To the best of our knowledge, this is the first report on the cafarsite crystal-structure after the study by Edenharter *et al.* (1977). We here present new chemical and structural data for this mineral and, on the basis of our results, we propose a new crystal-chemical formula and reinterpret the structural arrangement of cations in coordination polyhedra.

2. Experimental methods

2.1. Samples

Two cafarsite samples were examined in the present study. Both came from the same area Wanni glacier – Monte Cervandone, Binn Valley, Valais (CH) but they showed different morphological features. The first (hereafter labeled as cafarsite1) kindly provided by the Museum of Natural history of Bern, sample no. B6467, appears as nicely formed and well-crystalline shiny black cubo-octahedra with prevalent octahedral faces (Fig. 1a). In the second specimen (cafarsite2), cafarsite also occurs as big cubo-octahedral crystals with dull dark grey-brown pockmarked surface. If the surface is scratched off, the interior appears ochre yellow in color. In addition, smaller cubo-octahedra appear dark reddish-brown on the surface but the interior is also ochre yellow (Fig. 1b, c). An attempt to select single-crystal fragments from this

https://doi.org/10.1127/ejm/2018/0030-2756 0935-1221/18/0030-2756 $ 4.50

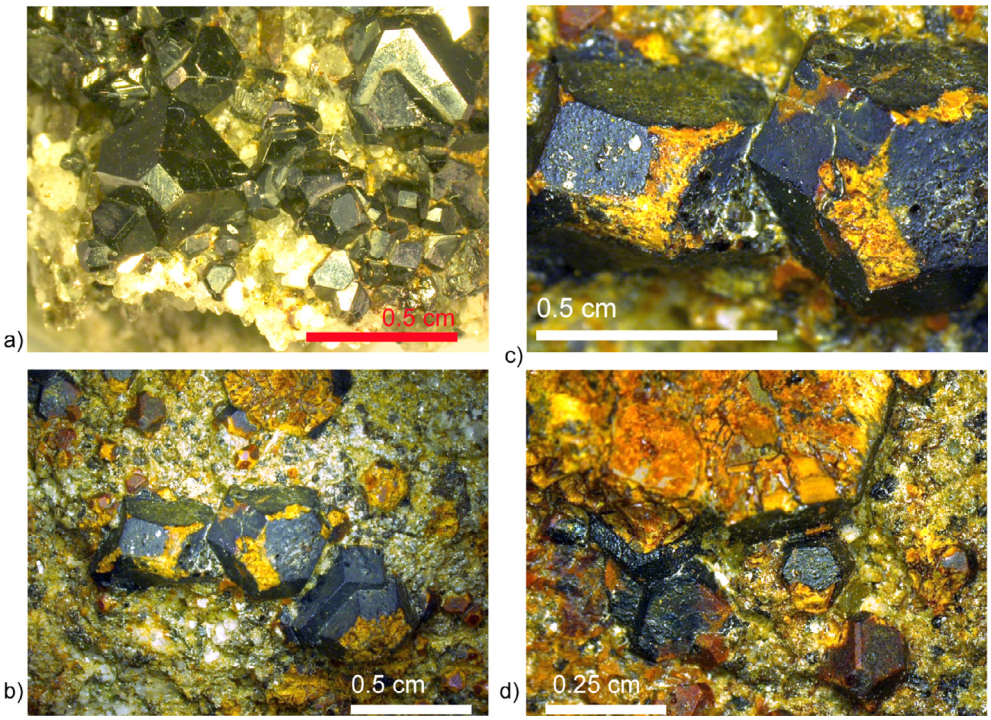

Fig. 1. Optical microscope pictures of cafarsite samples. (a) Cafarsite1 specimen used for structural and chemical investigation. Well-shaped cubo-octhaedral black crystals on quartz and clay minerals. (b) Cafarsite2 specimen: big dark-gray-brown and smaller reddish octahedral-shaped crystals. (c) Detail of two big crystals with partial scratched surface; (d) internal part of one of the big crystals scratched with a needle, showing the ochre yellow powder. (Online version in colour)

second specimen, either form the larger or from the smaller crystals, suitable for subsequent experiments, was not successful. As soon as the sample was scratched by a needle, the fragment decomposed to powder (Fig. 1d). Therefore, chemical analysis and structural investigation were performed on crystals belonging to the first specimen (cafarsite1).

2.2. Chemical analyses

The chemical composition of cafarsite1 sample was determined by electron microprobe analysis (EMPA) using a JEOL JXA-8230 instrument. The following analytical conditions were used: accelerating voltage 15 kV, beam current 20 nA, and beam diameter 1–10 μm. Standards were: wollastonite (Ca), rutile (Ti), corundum (Al), eskolaite Cr_2O_3 (Cr), $Ca_3(VO_4)_2$ (V), hematite (Fe), manganosite (Mn), periclase (Mg), albite (Na), cassiterite (Sn), GaAs (As), $(Zr,Y)O_2$ (Zr and Y), LaB_6 (La), CeB_6 (Ce), PrB_6 (Pr) and NdB_6 (Nd). The chemical formula of cafarsite was computed on the basis of 16.5 cations, that is, according to crystal symmetry, the total number of cations excluding the As content which was fixed to 14 atoms per formula unit (apfu, see Sect. 4). Such approach was based on the anomalous value of As content (always > 14.7 apfu) computed on the basis of 84.5 negative charges (84 due to oxygen plus 0.5 due to fluorine according to structural refinement, see next paragraph).

2.3. Single-crystal X-ray diffraction

A single crystal with dimension 0.16 mm × 0.10 mm × 0.10 mm was selected from the cafarsite1 specimen and glued on the tip of a glass fiber, mounted on a goniometer head. Diffraction data were collected at room temperature on a Bruker SMART APEX II CCD diffractometer equipped with a graphite-monochromatized Mo*K*α radiation (λ = 0.71069 Å). Frames were recorded with an ω-ϕ scan. Integration and correction for absorption were performed using the Apex 2v. 2011.4-1 software package.

Structure solution by direct methods (SHELXTL 2008, Sheldrick, 2008) indicated $Pn\bar{3}$ space group in agreement with previous results (Edenharter *et al.*, 1977). Structural refinement was done by using SHELXL 2013 (Sheldrick, 2015). Neutral atomic scattering factors were used and starting atomic coordinates were those reported by Edenharter *et al.* (1977) using origin choice 2 of space group $Pn\bar{3}$. Moreover, we recognized a new site that had all characteristics of a fluorine position. For this site we also tested refinement with oxygen scattering factors but the corresponding atomic displacement parameter U^{eq} converged to a value less than half of those of O1–O7. This test suggested too low assigned scattering power. Subsequent refinements with F scattering factors resulted in a corresponding U^{eq} value as observed for oxygen sites. In contrast to Edenharter *et al.* (1977), the Fe(1) site was refined with Ca scattering factors and renamed Ca3. Its occupancy

Table 1. Crystal data and refined parameters of cafarsite.

	Cafarsite1	Cafarsite1-A	Cafarsite1-B
Crystal data			
a (Å)	15.9614(2)	15.9675(3)	15.9574(2)
Cell volume (Å^3)	4066.43(15)	4071.1(2)	4063.37(15)
Z	4	4	4
Space group	$Pn\bar{3}$	$Pn\bar{3}$	$Pn\bar{3}$
Refined chemical formula*	$(Ca_{8.77}REE_{0.28}Na_{0.14}Mn_{0.31})_{\Sigma 9.5}$ $(Ti_{4.07}Fe_{2.83}Mn_{0.1})_{\Sigma 7}$ $(AsO_3)_{14}F_{0.5}$	$(Ca_{8.80}REE_{0.24}Na_{0.13}$ $Mn_{0.33})_{\Sigma 9.5}$ $(Ti_{4.16}Fe_{2.74}Mn_{0.1})_{\Sigma 7}$ $(AsO_3)_{14}F_{0.5}$	$(Ca_{8.47}REE_{0.26}Na_{0.55}Mn_{0.22})_{\Sigma 9.5}$ $(Ti_{4.38}Fe_{2.49}Mn_{0.1})_{\Sigma 7}$ $(AsO_3)_{14}F_{0.5}$
Crystal size (mm)	0.160 × 0.10 × 0.10	0.10 × 0.05 × 0.05	0.03 × 0.08 × 0.09
Calculated density (g/cm^3)	4.075	4.063	4.054
Absorption coeff. (mm^{-1})	14.554	14.501	14.419
Intensity measurement			
Diffractometer	APEX II SMART		
X-ray radiation	Mo*K*α λ = 0.71073 Å		
X-ray power	50 kV, 30 mA		
Monochromator	Graphite		
Temperature	25 °C	25 °C	25 °C
Time per frame	10 s	30 s	30 s
Max. 2θ	66.16°	61.77°	68.64°
Index ranges	$-23 \le h \le 24$ $-24 \le k \le 20$ $-24 \le l \le 24$	$-23 \le h \le 21$ $-23 \le k \le 23$ $-23 \le l \le 22$	$-25 \le h \le 24$ $-24 \le k \le 25$ $-21 \le l \le 21$
Reflections measured	89248	80527	45826
Unique reflections	2591	2162	2846
Observed reflections $I > 2\sigma(I)$	2174	1770	2338
Structure refinement			
Refined parameters	124	121	123
R(int)	0.0948	0.1103	0.0869
R(σ)	0.0265	0.0287	0.0342
GooF	1.082	1.069	1.035
*R*1, $I > 2\sigma(I)$	0.0217	0.0241	0.0228
*R*1, all data	0.0319	0.0380	0.0362
w*R*2 (on F^2)	0.0461	0.0456	0.0467
$\Delta\rho_{min}$ ($-$eÅ^{-3}) close to	−0.51 O7	−0.59 As2	−0.59 As3
$\Delta\rho_{max}$ (eÅ^{-3}) close to	0.92 Ca1A	0.79 Ca1	0.73 As3

converged to a value lower than 1 and was subsequently considered to be shared by Ca and Na. Strongly anisotropic atomic displacement parameters for Ca3 suggested disorder and the site was displaced from the special position of $x = ¼$ and refined at a split position (0.2367(3), ¾, ¾). The occupancy of the Ca1 site was refined with Ca and Sb. The Sb scattering factors were chosen to model the amount of REE at this site (*ca.* ⅔ *La* + ⅓ Y according to results of chemical analyses), which roughly corresponds to the electron number of Sb. The Ca1 site showed a nearby residual density that was refined as a low occupied Ca position (Ca1A) at 0.66(5) Å from Ca1. For the Ti1 and Fe2 sites, Ti *versus* Fe was refined.

Extinction correction was applied due to reduced values for strong F_o^2 at low diffraction angle (*e.g.* $hkl = 044$ and 008) compared to F_c^2. We also considered substantial multiple diffraction effects and thus collected the data with high redundancy (3.2 for full sphere). In spite of the high R_{int} value (=9%), the refinement converged to $R1 = 2.17\%$ (Table 1).

An additional crystal, cafarsite1-A, with smaller dimension (*ca.* 0.05 × 0.05 × 0.10 mm) was selected from the same specimen and measured by using the same strategy as reported above. However, also in this data set R_{int} was not reduced. Finally, to exclude an instrumental effect, diffraction data on a third crystal, cafarsite1-B, were collected by using a corresponding SMART APEX II CCD diffractometer installed at Shimane University. Although refinements of all three cafarsite crystals converged to good *R*1 values (Table 1), the intensity data were all characterized by a high value of R_{int}, indicating an intensity mismatch among equivalent reflections, most probably caused by the anisotropic influence of multiple diffraction in crystals of low mosaicity. Additional tests indicated that the intensity variation of reflections related by symmetry or measured under different diffracting orientations does not show any systematics and is thus not due to lower symmetry with associated twinning.

2.4. X-ray powder diffraction

Two powder-diffraction patterns were collected in order to analyze the cafarsite2 sample. One was collected from the scratched-off brownish cover using a PANalytical X'Pert Pro MPD diffractometer equipped with an XCelerator detector and a Cu anode. The powder was put onto a silicon plate and measured with an irradiated length of 10 mm from 5 to 75° 2θ with a time/step of 80 s. Phase identification was done with the HighScore Plus V4.6 software suite using the PDF-2004 database.

The second sample consisted of a ground cubo-octahedron. The resulting ochre-brownish powder was mixed with silicon (ratio *ca*. 3:1) and subsequently measured on a silicon plate with a PANalytical CubiX3 diffractometer equipped with a secondary beam monochromator, a Xe proportional detector and a Cu anode. Data were collected with an irradiated length of 10 mm from 5 to 75° 2θ with a time/step of 10 s. Lattice parameters of cafarsite were Pawley-refined using TOPAS-Academic V6 (Coelho, 2016) from this sample.

3. Results

3.1. Chemical composition

The chemical formula of cafarsite as computed from average EMPA data is reported in Table 2. At variance with previous studies (Edenharter *et al.*, 1977; Harris, 1989) our chemical analyses showed the occurrence of rare-earth elements (REE), mainly Ce and Y, and the absence of Al. The analyses obtained at different analytical points demonstrated that the chemical composition of the crystal is inhomogeneous (Fig. 2; Fig. S1 in Supplementary Material linked to this article and freely available at https://pubs.geoscienceworld.org/eurjmin).

3.2. Crystal structure

The atomic coordinates, equivalent displacement parameters and site occupancies of cafarsite1 are reported in Table 3; anisotropic displacement parameters in Table 4, deposited as part of the Supplementary Material, and selected interatomic distances in Table 5. The Cif file has been submitted as supplementary material.

The cafarsite structure is constituted by AsO_3 trigonal pyramids linked to MO_6 polyhedra with M = Ca, Mn, Fe, Ti (Edenharter *et al.*, 1977). In contrast to previous studies (Edenharter *et al.*, 1977) a new F site was located form the difference Fourier map. This site occupies a special position at (¼, ¼, ¼) and bonds to four Ca1 sites at 2.4152(11) Å, forming a pseudo-tetrahedron around F. The $MO_{6–8}$ polyhedra are connected to the AsO_3 trigonal pyramids (Fig. 3). The Ca1 site is seven-fold coordinated to 6 O sites (3 × O7 and 3 × O2) and one F, not detected in previous structural refinement (Edenharter *et al.*, 1977). Three additional bonds to O7 also occur at longer distances (3.023(2) Å, Table 5). The short distance between Ca1 and the low-occupancy subsite Ca1A detected close to it required that the total occupancy of both sites had to be fixed at 1.

Table 2. Chemical composition of cafarsite. Average, minimum and maximum values of 18 analytical points are reported. Formula coefficients (*apfu*) were computed on the basis of 16.5 cations (excluding As).

Wt%	Average	Min	Max		*apfu*
TiO_2	11.91	10.39	13.15	Ti	3.91
V_2O_3	0.07	0.00	0.15	V^{3+}	0.02
FeO	8.06	6.87	10.04	Fe	2.94
MnO	1.62	1.19	3.04	Mn^{2+}	0.60
CaO	16.65	15.38	17.50	Ca	7.79
Na_2O	0.95	0.64	1.15	Na	0.81
SnO_2	0.12	0.04	0.19	Sn	0.02
As_2O_3	56.87	56.01	57.56	As^{3+}	14
Y_2O_3	0.56	0.23	1.04	Y	0.13
La_2O_3	0.17	0.00	0.41	La	0.03
Ce_2O_3	0.95	0.55	1.57	Ce	0.15
Pr_2O_3	0.15	0.02	0.33	Pr	0.02
Nd_2O_3	0.46	0.21	0.89	Nd	0.07
Total	98.56				

The Ca2 and Ca3 sites are eight-fold coordinated. Ca3 corresponds to the Fe(1) site in Edenharter *et al.* (1977) who originally described it as a highly unusual four-fold (4 × O4) coordinated Fe site. However, in addition to the four Ca3–O4 bonds of *ca*. 2.2 Å, four additional O5 sites at bond distances of 2 × 2.616(5) and 2 × 2.992(5) Å have to be accounted to the coordination. Ca3 resembles the dodecahedral X site in a garnet structure with the central cation displaced parallel to the long Ca3–O5 bonds (Fig. 4). With the exception of the new low-occupancy Ca1A site contributing to Ca1, all the other crystallographic positions are fully occupied (Table 3). The chemical analyses indicated that Ca is substituted by REE (Fig. 2b). Test refinements of Ca *vs* REE at the Ca1, Ca2, and Ca3 sites showed that only Ca1 bears *ca*. 14% REE. Small amounts of Mn (*occ.* = 0.052(7)) and Na (*occ.* = 0.047(7)) were assumed at Ca2 and Ca3, respectively (Table 3). The octahedral sites Ti1 and Fe2 are mainly occupied by Ti with subordinate Fe whereas Mn1 is occupied by Mn^{2+} and possibly Fe^{2+} (Table 3). The dense arrangement of cations and anions in the cafarsite structure does not provide sufficient space for H_2O molecules. Thus, the hydrous character of cafarsite (Edenharter *et al.*, 1977) is not supported by our structural data.

3.3. X-ray powder diffraction

The X-ray diffraction pattern collected from the bulk of dark cubo-octahedral cafarsite2 crystals indicated that they had transformed to a high extent to an amorphous material. Rietveld quantification was very unreliable due to the heavily oriented sample on the silicon plate; from the mixture of 1 part Si and 3 parts of the ground dark cubo-octahedra, it can be estimated that only a very low amount of crystalline cafarsite was remaining. The Pawley-refined unit-cell size (a = 15.9649(4) Å) of cafarsite2 (Fig. 5) is, however, identical to the one of the cafarsite1 sample.

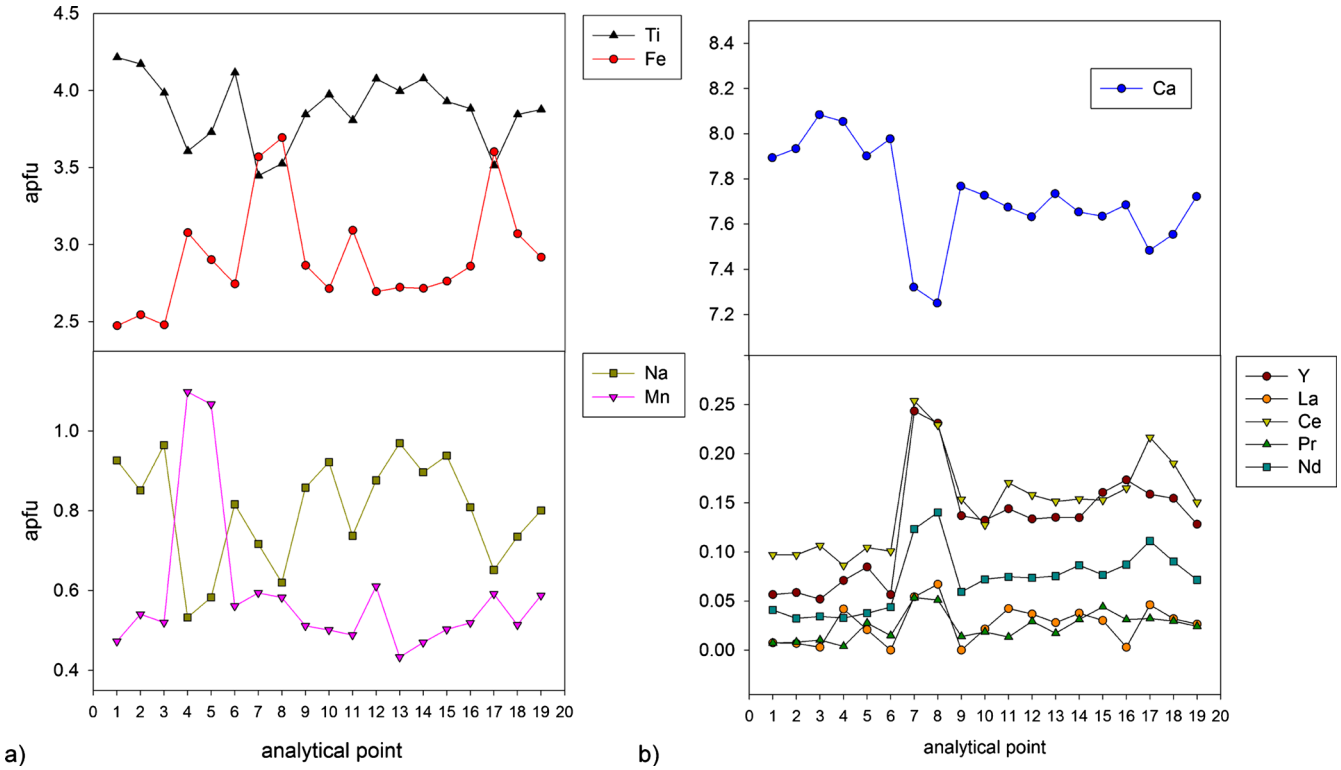

Fig. 2. Chemical composition (apfu) of cafarsite1 at different analytical points as collected by EMPA. (Online version in colour)

Table 3. Atomic coordinates, U^{eq} (Å^2), and occupancies of cafarsite1.

Site	*x*	*y*	*z*	U^{eq}	Occ.
As1	0.37637(2)	0.37637(2)	0.37637(2)	0.00830(8)	1 As
As2	0.22955(2)	0.97760(2)	0.03846(2)	0.00798(6)	1 As
As3	0.39313(2)	0.64037(2)	0.35266(2)	0.01081(6)	1 As
Ca1	0.16264(4)	0.16264(4)	0.16264(4)	0.0118(3)	0.828(3) Ca, 0.144(3) Sb
Ca1A	0.1387(18)	0.1387(18)	0.1387(18)	0.011(9)	0.029(6) Ca
Ca2	0.09372(3)	0.62580(3)	0.35566(3)	0.00984(12)	0.948(7) Ca, 0.052(7) Mn
Ca3	0.2367(3)	¾	¾	0.0240(12)	0.453(7) Ca, 0.047(7) Na
Ti1	0.95160(3)	¾	¼	0.00678(14)	0.596(10) Ti, 0.404(10) Fe
Fe2	−0.00682(3)	¼	¼	0.00701(14)	0.240(10) Fe, 0.760(10) Ti
Mn1	0	0	0	0.00984(16)	1 Mn
F	¼	¼	¼	0.0139(10)	1 F
O1	−0.00583(10)	0.98055(10)	0.13795(11)	0.0117(3)	1 O
O2	0.30984(11)	0.00357(10)	0.36011(10)	0.0114(3)	1 O
O3	0.28780(11)	0.63317(10)	0.04817(11)	0.0121(3)	1 O
O4	0.16235(11)	0.73719(10)	0.14148(11)	0.0138(3)	1 O
O5	0.17380(13)	0.59431(14)	0.22196(13)	0.0306(5)	1 O
O6	0.03326(10)	0.66526(10)	0.22544(10)	0.0121(3)	1 O
O7	0.17348(12)	0.41758(12)	0.21345(11)	0.0190(4)	1 O

The dark surface associated with cafarsite2 consists mainly of the arsenate-hydrates kankite ($FeAsO_4 \cdot 3.5H_2O$, PDF No. 00-029-0694) and parasymplesite ($Fe_3(AsO_4)_2 \cdot 8H_2O$, PDF No. 00-035-0461), and magnetite. Quartz and the sheet silicates are most likely originating from the host-rock matrix. No cafarsite reflections were detected in this diffraction pattern (Fig. S2 in Supplementary Material).

4. Discussion

4.1. Chemical variation of cafarsite

In the structure of cafarsite three sites, Ca1, Ca2, and Ca3, host 9.5 cations (mainly occupied by Ca with minor amount of REE, Na, and Mn) whereas the remaining 7 cations

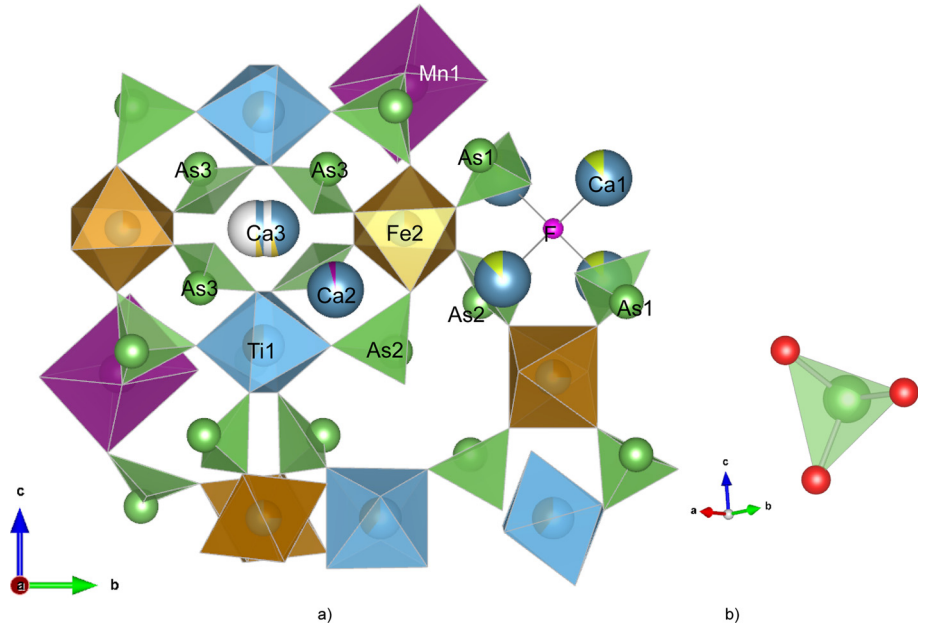

Fig. 3. (a) Fragment of the cafarsite crystal-structure emphasizing the connection between different polyhedra. Site occupancies are shown by partially colored sites. (b) AsO_3 trigonal pyramid: oxygen atoms are represented as red spheres. (Online version in colour)

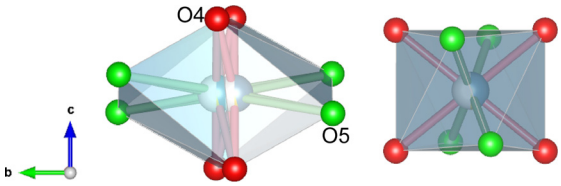

Fig. 4. Projection along **a** of the coordination polyhedron around the Ca3 site: two orientations occurring in the unit cell are shown to highlight the splitting of the Ca3 site along the axial directions (left picture), and (right picture) the coordination resembling the one of the X site in the garnet structure. O4 and corresponding Ca3–O4 bonds are shown in red; O5 and Ca3–O5 bonds in green. The occupancy of the Ca3 site is shown as partially colored sphere. (Online version in colour)

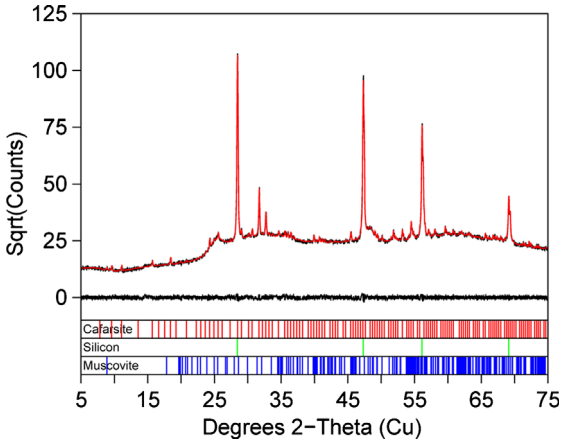

Fig. 5. X-ray powder diffraction pattern of the bulk of the cafarsite2 specimen. (Online version in colour)

(Ti, Fe, and Mn) are distributed at three octahedral sites Ti1 (3 pfu), Fe2 (3 pfu), and Mn1 (1 pfu). This is consistent with results of chemical analyses and a simplified average empirical formula can be written as $(Ca_{7.8}Na_{0.8}Mn_{0.5}REE_{0.4})_{\Sigma 9.5}(Ti_{3.9}Fe^{3+}{}_{2.1}Fe^{2+}{}_{0.9}Mn^{2+}{}_{0.1})_{\Sigma 7}(AsO_3)_{14}F_{0.5}$ (Table 2). Charge balance is obtained by optimizing the Fe^{2+}/Fe^{3+} ratio. Nevertheless, it should be borne in mind that the material is inhomogeneous and additional substitutions may occur. In particular, the Fe and Ti content are related by an inverse trend (Fig. 2a), *i.e.* low Ti content is balanced by the increase of Fe and *vice versa*. Fe *versus* Ti apfu is plotted in Fig. 6 yielding the regression line (1) $Ti = -0.57(6)Fe + 5.55(18)$ ($R = 92\%$). A similar correlation (same coefficients within errors) was also obtained by plotting the (Fe + Mn) *versus* Ti contents ($Ti = -0.49(4)Fe + 5.58(15)$, $R = 94\%$).

As derived from the regression equation (1) the maximum value of Ti amounts to *ca.* 5 apfu if Fe is not replacing Ti. This leads to the simplified chemical composition $Ca_{9.5}(Ti_5Fe_2)_{\Sigma 7}(AsO_3)_{14}F_{0.5}$ (ignoring that Ca may be substituted by REE, Mn and Na). For this composition, the total number of negative charges is 84.5 of which 42 are balanced by As^{3+} and 19 by Ca^{2+}. For charge balance, 23.5 additional positive charges are needed; 5 Ti^{4+} contribute 20 charges and 2 Fe^{2+} additional 4, leading to a surplus of 0.5 positive charges (sum = 24 positive charges). Thus, the suggested formula is not charge neutral. A charge balanced composition without any additional heterovalent substitution requires slight modification to $Ca_{9.5}(Ti_{4.75}Fe^{2+}{}_{2.25})_{\Sigma 7}(AsO_3)_{14}F_{0.5}$.

According to EMPA data the minimum number of Ti is 3.5 apfu corresponding to the simplified chemical formula $Ca_{9.5}(Ti_{3.5}Fe_{3.5})_{\Sigma 7}(AsO_3)_{14}F_{0.5}$, which becomes charge balanced by a combination of ferric and ferrous iron: $Ca_{9.5}(Ti_{3.5}Fe^{3+}{}_{2.5}Fe^{2+})_{\Sigma 7}(AsO_3)_{14}F_{0.5}$. This formula is

Table 5. Selected bond-distances (Å) of cafarsite1.

As1–O7 × 3	1.7667(17)	Ca2–O1	2.3274(17)
		Ca2–O6	2.3766(17)
As2–O1	1.7499(17)	Ca2–O3	2.4384(18)
As2–O2	1.7855(16)	Ca2–O4	2.4465(17)
As2–O3	1.7963(16)	Ca2–O1	2.5159(17)
		Ca2–O5	2.538(2)
As3–O6	1.7585(16)	Ca2–O2	2.5765(18)
As3–O5	1.761(2)	Ca2–O3	2.6576(18)
As3–O4	1.7835(17)		
Ca1–O7 × 3	2.3625(19)	Ca3–O4 × 2	2.2264(18)
Ca1–F	2.4152(11)	Ca3–O4 × 2	2.265(2)
Ca1–O2 × 3	2.6021(18)	Ca3–O5 × 2	2.616(5)
Ca1–O7 × 3	3.023(2)	Ca3–O5 × 2	2.992(5)
Ca1A–O2 × 3	2.308(16)	Ti1–O6 × 2	1.9188(16)
Ca1A–O7 × 3	2.59(2)	Ti1–O3 × 2	1.9600(16)
		Ti1–O4 × 2	2.0509(17)
Fe2–O5 × 2	1.9053(19)		
Fe2–O7 × 2	1.9649(17)	Mn1–O1 × 6	2.2255(17)
Fe2–O2 × 2	2.0071(16)		

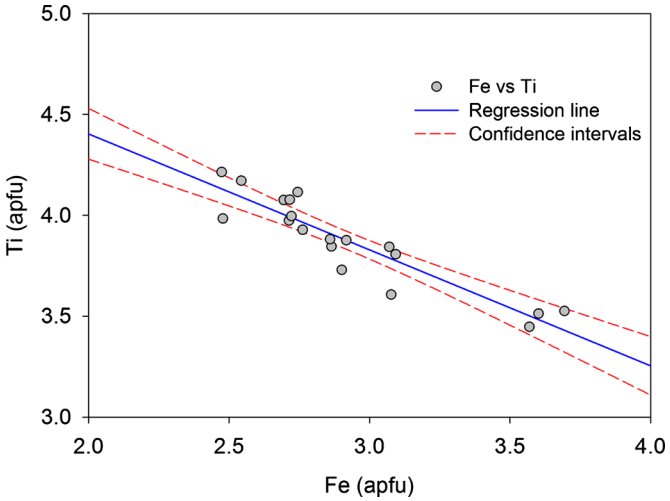

Fig. 6. Plot of Fe *vs*. Ti content (in apfu). Calculated regression line (Ti = −0.57Fe + 5.55, R = 92%) with corresponding confidence interval (0.05) is also shown. (Online version in colour)

also supported by the structural data because bond distances suggest six small octahedra pfu (Ti1, Fe2) suitable for Ti^{4+} and Fe^{3+} plus one larger octahedron pfu (Mn1), ideal for Mn^{2+} and Fe^{2+}. One might also predict a hypothetical end-member formula with only ferric iron of the type $Ca_{9.5}(Ti_{2.5}Fe^{3+}_{4.5})_{\Sigma 7}(AsO_3)_{14}F_{0.5}$, which is not supported by the structural data because of the observed size difference between (Ti1, Fe2) and Mn1 octahedra.

The Ca dominant sites Ca1 (2 pfu), Ca2 (6 pfu), Ca3 (1.5 pfu) with coordination numbers of 7, 8, and 8, respectively, show a complex substitution pattern with additional Na, REE, and possibly Mn. The REE content (Krzemnicki, 1993) is not surprising as other REE type-locality minerals from this occurrence are the arsenite cervandonite-(Ce), the arsenates paraniite-(Y) and gasparite-(Ce), and the oxalate deveroite-(Ce), see also Guastoni *et al.* (2006). One would expect that REE^{3+} incorporation at Ca sites (Fig. 2) follows the equation $REE^{3+}+Na \rightarrow 2\ Ca$. However, the observed compositional variations (Fig. 2) do not support this model. Actually, the analytical points with highest REE content (points 7 and 8 in Fig. 2) show no enrichment in Na. Thus, we assume that charge balance for REE incorporation is regulated *via* a combination of decreased Ti content and the ferrous/ferric ratio at the octahedral sites (Fig. 2). In addition, the Na content in cafarsite, which varies between *ca*. 0.5 and 1 Na apfu, shows a slight positive correlation with the Ti concentration at the octahedral sites. Thus, in Ti-rich compositions the high charge of Ti^{4+} is partly balanced by Na at the Ca dominant sites.

4.2. Significance and limitation of site-occupancy refinements for cafarsite

The structure refinement indicated that As sites are fully occupied yielding 14 As pfu and the total number of cations, excluding As atoms, is 16.5 apfu. However, our chemical analyses systematically showed an As content higher than 14 apfu (14.79–15.09 apfu calculated on the basis of 84.5 negative charges). Several attempts to determine whether the additional As could be located at other crystallographic positions partially replacing other cations were unsuccessful: all polyhedra show bond-distances too long for As, moreover, As^{3+} is expected to be three-fold coordinated and there was no indication of residual density or anomalous atomic displacement parameters of other metals (Table 4). Tetrahedral sites as possible source of AsO_4 groups do not exist in cafarsite. Therefore, we are convinced that the estimated amount of As is affected by a systematic overestimation in our EMP analysis.

X-ray diffraction cannot distinguish between Mn and Fe due to similar atomic number; therefore, although the Mn1 site was refined with Mn scattering factors suggested by the Mn1–O mean bond length, it has to be considered as partially occupied by both Fe and Mn. The refined Mn content in cafarsite1 is equal to 1.31 apfu; 0.31 apfu are at the Ca2 site (Table 3), the remaining 1 apfu at the Mn1 site. However, part of this 1 apfu at Mn1 are Fe atoms; we attributed 0.10 apfu Mn and 0.9 apfu Fe to Mn1 (Table 6), which led to a total Fe content of 2.83 apfu, in agreement with the average chemical composition. The same approach, to estimate the refined amount of Fe apfu, was used for the crystals cafarsite1-A and B (Table 1). Nevertheless, this approach is obviously arbitrary considering the inhomogeneous composition of the sample.

The variability of the chemical composition is in agreement with the different concentrations of specific cations estimated by structural refinement in the two crystals cafarsite1 and cafarsite1-B (Table 1). The small crystal (cafarsite1-A) was picked up from the same fragment of cafarsite1 and did not show any significant difference in terms of refined cation content.

Table 6. Refined site scattering (*epfu*) of cafarsite1 and cafarsite1-B and site population (*apfu*) calculated according to the average chemical composition reported in Table 2.

Site	Site multiplicity	Cafarsite-1			Cafarsite1-B		Assigned site population (*apfu*) EMPA	Calculated site scattering
		Scattering species	Refined site scattering (SC-XRD)*		Scattering species	Refined site scattering (SC-XRD)*		
As1	8e	As	66		As	66	2 As	66
As2	24h	As	198		As	198	6 As	198
As3	24h	As	198		As	198	6 As	198
Ca1 + Ca1A	8e	0.86Ca + 0.14Sb	34.4 + 14.28 = 48.68		0.86Ca + 0.13Sb	34.4 + 13.26 = 47.7	1.79Ca + 0.13Y + 0.15Ce + 0 . 0 3 L a + 0 . 0 2 P r + 0.07Nd 0.02V + 0.02Sn	35.8 + 5.07 + 8.7 + 1.71 + 1.18 + 4.2 + 0.46 + 1 = 58.1
Ca2	24h	0.95Ca + 0.05Mn	114 + 7.5 = 121.5		0.97Ca + 0.03Mn	116.4 + 4.5 = 120.9	5.7 Ca + 0.3 Mn	114 + 7.5 = 121.5
Ca3	12f	0.45Ca + 0.05Na	13.5 + 0.83 = 14.33		0.32Ca + 0.19Na	9.6 + 3.14 = 12.74	0.3 Ca + 0.81Na	6 + 8.91 = 14.91
			∑ = 184.51			∑ = 181.34		∑ = 194.51
Ti1	12g	0.60Ti + 0.40Fe	39.6 + 31.2 = 70.8		0.64Ti + 0.36Fe	42.24 + 28.08 = 70.32	1.8Ti + 1.3Fe	39.6 + 33.8 = 73.4
Fe2	12f	0.24Fe + 0.76Ti	18.72 + 50.16 = 68.88		0.18Fe + 0.82Ti	14.04 + 54.12 = 68.16	0.94Fe + 2.11Ti	24.44 + 46.42 = 70.86
Mn1	4b	1Mn	25		1Mn	25	0.1Mn + 0.2Fe + 0.7Fe	7.5 + 18.2 = 25.7
			∑ = 164.68			∑ = 163.48		∑ = 169.96
Total**			∑ = 349.19			∑ = 344.82		∑ = 364.47

* For a better comparison to chemical formula (*apfu*) site scattering was computed considering ¼ multiplicity, ** Total site scattering of Ca and octahedral sites.

The refined site occupancies in cafarsite1-A and cafariste1-B showed variable amount of Ca and Na at the Ca3 site, and of Ti and Fe at Ti1 and Fe2 sites, respectively. In particular, the cafarsite1 sample has less Na (0.14 apfu) and Ti (4.07 apfu) compared to cafarsite1-B (0.55 Na apfu and 4.38 Ti apfu). As already discussed, Fe and Ti are related by an inverse trend. A similar relation between the Na and Ca concentration cannot be found. The calcium concentration decreases with increasing REE content (Fig. 2b). Interestingly, the amount of Na estimated by structural refinement was found to be much lower (0.14 and 0.13 apfu for cafarsite1 and cafarsite1-A sample, respectively) than that estimated by chemical analyses (mean value = 0.81 apfu and minimum value = 0.53 apfu) (Table 2). Similarly, the refined content of Ca apfu was always higher than the maximum value provided by EMPA. This mismatch is a consequence of the complex composition at the Ca1 site. For a chemically heterogeneous crystal, there are several potential occupants at Ca1: Ca, Na, Y, *La*. Even if the combined scattering of Y and *La* was modelled by Sb as dummy species, there remains a three-variable problem (Ca, Na, and Sb), which cannot be solved without fixing one of the parameters. In our model Na was set at zero. Consequently, for a given scattering power at this site, the presence of additional Na would increase the REE and decrease the Ca content. As an example: fixing 0.33 Na at Ca1 refines to 0.2 Sb (REE) and 0.47 Ca. Thus, the Ca-dominant sites (Ca1–Ca3) add up to the composition $(Ca_{7.98}Na_{0.78}\ REE_{0.43}Mn_{0.31})_{\Sigma 9.5}$ pfu, which is close to the mean composition.

The best highly simplified formula of cafarsite is $Ca_{9.5}(Ti_{3.5}Fe^{3+}{}_{2.5}Fe^{2+})_{\Sigma 7}(AsO_3)_{14}F_{0.5}$ with partial substitution of Mn^{2+} for Fe^{2+} and Ca, additional incorporation of Ti for Fe^{3+} combined with Na substitution at Ca dominant sites and variations in the ferric/ferrous ratio for charge balance. REE at Ca dominant sites seem to be associated with low Ti and increased Fe.

4.3. General differences to the previous studies

The results here presented show several differences to the previous description of cafarsite (Edenharter *et al.*, 1977) from both chemical and structural perspective. A comparison between the analyses of different cafarsite samples from the same locality as our sample (Edenharter *et al.*, 1977; Harris, 1989) (Table 7) confirmed the significant variability of the chemical composition. In contrast, the sample from the Hemlo deposit (Harris, 1989) differs significantly from the others because of high Mn and V content. If the previous cafarsite analyses (Edenharter *et al.*, 1977; Harris, 1989) are normalized to 30.5 cations as established in our structure refinements, the AsO_3 values vary between 13.76 and 14.31 pfu (Table 7). This reassures that the structure contains 14 AsO_3 pfu and that our As_2O_3 content (EMPA) is systematically too high.

On the basis of our new results, we conclude that there is no H_2O in the cafarsite structure. We located a new anion site (F) and considered it occupied by fluorine, though the

Table 7. Comparison of chemical composition of cafarsite samples from Hemlo deposit (Ontario, Canada) and from Monte Cervandone (Binn Valley, Valais, Swiss/Italian border).

wt%	Hemlo[a]	Italy[a]	Switzerland[a]	Cafarsite[b]	Cafarsite1[*]
TiO_2	11.5	13.4	11.5	14.1	11.91
V_2O_3	4.7	–	–	–	0.07
FeO	2.3	7.9	8.2	7.8	8.06
Al_2O_3	0.7	–	–	0.7	–
MnO	6.3	2.6	5.1	2.6	1.62
CaO	17.9	17.6	17.6	16.5	16.65
Na_2O	–	–	–	1.1	0.95
SnO_2	–	–	–	0.13	0.12
As_2O_3	53.3	55.2	54.5	55.0	56.87
Y_2O_3	–	–	–	–	0.56
La_2O_3	–	–	–	–	0.17
Ce_2O_3	–	–	–	–	0.95
Pr_2O_3	–	–	–	–	0.15
Nd_2O_3	–	–	–	–	0.46
Total	96.7	96.7	97.9	97.93	98.56
	apfu on 30.5 cations				*apfu* on 16.5 cations
Ti	3.67	3.67	4.30	4.40	3.91
V^{3+}	1.60	–	–	–	0.02
Fe	0.80	2.92	2.83	2.71	2.94
Al	0.37	–	–	–	–
Mn^{2+}	2.25	1.83	0.95	0.91	0.60
Ca	8.12	8.02	8.10	7.34	7.79
Na	–	–	–	0.89	0.81
Sn	–	–	–	0.02	0.02
As^{3+}	13.68	14.05	14.31	13.88	14
Y	–	–	–	–	0.13
La	–	–	–	–	0.03
Ce	–	–	–	–	0.15
Pr	–	–	–	–	0.02
Nd	–	–	–	–	0.07

[a] Harris (1989).
[b] Edenharter *et al.* (1977).
[*] This study; cation basis without As^{3+}

low F content cannot be revealed by EMPA. Interpretation of this site as OH group or H_2O molecule is excluded: the F site is surrounded by four Ca atoms at 2.4152(11) Å; the only oxygen available as possible hydrogen-bond acceptor would be O7 (at 2.998 Å from F). However, there would not be enough space for a proton between F and O7 because of the close distance to Ca1 sites (Fig. 7). In addition, the F site is at ¼, ¼, ¼ of site symmetry 23 requiring that any potential H had to be disordered over 12 sites at general position. Furthermore, application of oxygen scattering factors for the F site caused an unreasonable atomic displacement parameter.

The original suggestion of cafarsite as a hydrous species (Graeser, 1966; Edenharter *et al.*, 1977) is based on independent chemical analyses yielding between 1.6 and 3 wt% H_2O. Edenharter *et al.* (1977) admitted that structural data and chemical analyses were not collected on the same material. The infra-red spectrum (no. 087) of a cafarsite sample (KBr pellet) from Monte Cervandone (Chukanov, 2014) shows a weak and diffuse H_2O specific band at 3325 cm^{-1} associated with the bending mode at 1640 cm^{-1}, probably related to humidity of the KBr pellet. An additional cafarsite spectrum (no. 094) from

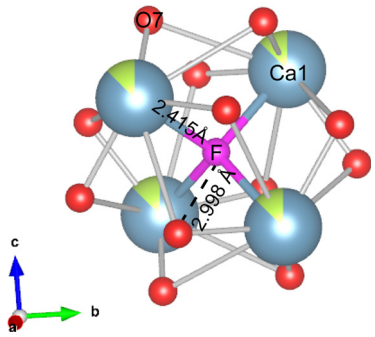

Fig. 7. Coordination of F site (pink sphere) in the cafarsite structure. Oxygen atoms (O7) are shown as red spheres. The Ca1 site is reported as two-colored sphere to indicate partial occupancy by Ca and REE. Gray and two-colored cylinders represent the Ca–O and F–Ca bonds, respectively. (Online version in colour)

the same locality (Chukanov, 2014) exhibits considerably stronger diffuse H_2O absorptions, additional bands, and a different intensity distribution in the low wave-number range. We interpret this spectrum as related to a strongly altered sample. The Raman spectrum (ID R080118) reported in the RRUFF database (Lafuente *et al.*, 2015)

does not show any bands associated with OH/H_2O. All three spectra were collected on reddish-brown crystals. According to our study those crystals represent most likely altered cafarsite for which increased water content is expected. The lack of H_2O-related bands in the RRUFF Raman spectrum, assuming that the sample is slightly altered, is probably due to the lower sensitivity of this technique for minor H_2O content in minerals with high concentrations of heavy elements. The Raman spectra discussed by Kloprogge & Frost (1999) and Frost & Bahfenne (2010) are confined to the region below 1000 cm^{-1} and are in this range consistent with the spectrum in the RRUFF data base.

Our diffraction experiments on cafarsite2, yielding very high concentrations of X-ray amorphous altered material, may indicate that the assumed H_2O content (Graeser, 1966; Edenharter *et al.*, 1977) is confined to such alteration products. Identical cell dimensions for well crystalline (cafarsite1) material and for relict cafarsite within the amorphous transformed cafarsite2 suggest that during the decomposition process a different "H_2O-bearing cafarsite" was not formed.

Edenharter *et al.* (1977) presented a structural model in which all metal sites, including AsO_3 pyramids, are only partly occupied. This result is certainly caused by severe correlation between the site occupancies of metal sites and the scale factor and appears crystal chemically "highly unusual". In our new model, all major cation sites, not subject of splitting, are fully occupied. The definition of a Fe site with essentially planar four-fold coordination (Edenharter *et al.*, 1977) is also rated "highly unusual". The structural data indicate that four additional more remote O positions must be accounted to the coordination sphere, leading to eight-fold coordination (Ca3) resembling the X site in the garnet structure.

Acknowledgements: We are thankful to Beda Hofmann of Natural History Museum of Bern who kindly provided the cafarsite sample.

References

Chukanov, N.V. (2014): Infrared spectra of mineral species. Extended library, Vol. 1. Springer Dordrecht, Heidelberg, New York, 1726 p.

Coelho, A.A. (2016): TOPAS academic version 6. Coelho software. BRUKER-AXS, Brisbane, Australia.

Edenharter, A., Nowacki, W., Weibel, M. (1977): Zur Struktur und Zusammensetzung von Cafarsit: cafarsit ein As(III)-Oxid, kein Arsenat. *Schweiz. Mineral. Petr. Mitt.*, **57**, 1–16.

Frost, R.L. & Bahfenne, S. (2010): Raman spectroscopic study of the arsenite minerals leiteite $ZnAs_2O_4$, reinerite $Zn_3(AsO_3)_2$ and cafarsite $Ca_5(Ti,Fe,Mn)_7(AsO_3)_{12}$ $4H_2O$. *J. Raman Spectrosc.*, **41**, 325–328.

Graeser, S. (1966): Asbecasit und Cafarsit, zwei neue Mineralien aus dem Binnatal (Kt. Wallis). *Schweiz. Mineral. Petr. Mitt.*, **46**, 367–375.

Guastoni, A., Pezzotta, F., Vignola, P. (2006): Characterization and genetic inferences of arsenates, sulfates and vanadates of Fe, Cu, Pb, Zn from Mount Cervandone (Western Alps, Italy). *Period. Mineral.*, **75**, 141–150.

Harris, D.C. (1989): The mineralogy and geochemistry of the Hemlo gold deposit, Ontario. Geological Survey of Canada. *Econ. Geol. Rep.*, **38**, 88 p.

Kloprogge, J.T. & Frost, R.L. (1999): Raman spectroscopy study of cafarsite. *App. Spectrosc.*, **53**, 874–880.

Krzemnicki, M. (1993): Rare earth element-zoning in cafarsite from the Binnatal region (Switzerland). Rare Earth Mineral Conference. London, 63.

Lafuente, B., Downs, R.T., Yang, H., Stone, N. (2015): The power of databases: the RRUFF project. *in* "Highlights in Mineralogical Crystallography". T. Armbruster & R.M. Danisi, eds. W. De Gruyter, Berlin, Germany, 1–30.

Sheldrick, G.M. (2008): Crystal structure refinement with *SHELX*. *Acta Cryst.*, **A64**, 112–122.

— (2015): Crystal structure refinement with *SHELX*. *Acta Cryst.*, **C71**, 3–8.

Received 30 August 2017
Modified version received 24 October 2017
Accepted 24 October 2017